Rhamm$^{-/-}$ fibroblasts are defective in CD44-mediated ERK1,2 motogenic signaling, leading to defective skin wound repair

Cornelia Tolg,[1] Sara R. Hamilton,[1,2] Kerry-Ann Nakrieko,[3] Fatemeh Kooshesh,[5] Paul Walton,[3] James B. McCarthy,[6] Mina J. Bissell,[7] and Eva A. Turley[1,2,4]

[1]London Regional Cancer Program, London, Ontario N6A 4L6, Canada
[2]Department of Biochemistry, [3]Department of Anatomy and Cell Biology, and [4]Department of Oncology, University of Western Ontario, London, Ontario N6A 5B8, Canada
[5]Connective Tissue Research Group, Mount Sinai Hospital, Toronto, Ontario M5G 1X5, Canada
[6]Department of Laboratory Medicine and Pathology and Comprehensive Cancer Center, University of Minnesota, Minneapolis, MN 55455
[7]Life Sciences Division, Lawrence Berkeley National Laboratory, Berkeley, CA 94720

Rhamm (receptor for hyaluronan-mediated motility) is an hyaluronan binding protein with limited expression in normal tissues and high expression in advanced cancers. To understand its physiological functions and identify the molecular mechanisms underlying these functions, we created mice with a genetic deletion of Rhamm. We show that Rhamm$^{-/-}$ fibroblasts fail to resurface scratch wounds >3 mm or invade hyaluronan-supplemented collagen gels in culture. We identify a requirement for Rhamm in the localization of CD44 to the cell surface, formation of CD44–ERK1,2 (extracellular-regulated kinase 1,2) complexes, and activation/subcellular targeting of ERK1,2 to the cell nucleus. We also show that cell surface Rhamm, restricted to the extracellular compartment by linking recombinant protein to beads, and expression of mutant active mitogen-activated kinase kinase 1 (Mek1) are sufficient to rescue aberrant signaling through CD44–ERK1,2 complexes in Rh$^{-/-}$ fibroblasts. ERK1,2 activation and fibroblast migration/differentiation is also defective during repair of Rh$^{-/-}$ excisional skin wounds and results in aberrant granulation tissue in vivo. These results identify Rhamm as an essential regulator of CD44–ERK1,2 fibroblast motogenic signaling required for wound repair.

Introduction

To date, a physiological function for Rhamm (receptor for hyaluronan [HA]-mediated motility) has remained elusive. Analyses of animal models demonstrated instructive roles of Rhamm in tumorigenesis and inflammatory diseases (Tolg et al., 2003; Nedvetzki et al., 2004; Zaman et al., 2005), consistent with evidence for a role of Rhamm in motility and proliferation/apoptosis in culture (Turley et al., 2002; Adamia et al., 2005). However, given that migration and proliferation/apoptosis are essential functions for morphogenesis and tissue homeostasis, it is surprising that genetic deletion of Rhamm does not affect embryogenesis or adult homeostasis.

Rhamm was originally isolated from subconfluent fibroblasts in culture (Turley, 1982) and subsequently cloned from mesenchymal cells (Hardwick et al., 1992). Antibodies prepared against a shed form of Rhamm blocked HA-stimulated fibroblast motility, suggesting that Rhamm is a cell surface protein able to transduce motogenic signaling in culture (Turley et al., 2002). Rhamm-bound HA was detected in cancer cell lines and shown also to occur in intracellular compartments/structures, including the cytoskeleton, nucleus, and cytoplasm (Hascall et al., 2004; Adamia et al., 2005). These results suggest that Rhamm has both extracellular and intracellular functions. However, the role of Rhamm as a cell surface HA receptor became controversial partly because cloning of the human (Wang et al., 1996; Hofmann et al., 1998; Crainie et al., 1999) and mouse genes (Hofmann et al., 1998) revealed an absence of both a signal peptide required for export through the Golgi/ER and membrane spanning domains common to most cell surface receptors. We now know that Rhamm resembles a group of intracellular proteins that also lack these signature characteristics of classical cell surface proteins but that are nevertheless found

Figure 1. **Migration and invasion of Rhamm$^{-/-}$ fibroblasts are impaired.** (A) Migration into scratch wounds in 2D cultures (16 h). Significantly more Wt than Rh$^{-/-}$ fibroblasts migrate into 3-mm wound gaps in response to serum. Mean and SEM; $n = 6$ randomly chosen areas. Wt fibroblasts migrate at a higher speed and for longer distances than Rh$^{-/-}$ fibroblasts. Mean and SEM; $n = 30$ cells. One of six experiments is shown. (B) Invasion into collagen gels (48 h). Diagram of a collagen gel invasion assay constructed with HA and PDGF in the central plug. A significantly greater number of Wt than Rh$^{-/-}$ fibroblasts migrate into the plug. Mean and SEM; $n = 4$ randomly chosen areas. One of six experiments is shown. *, $P < 0.05$.
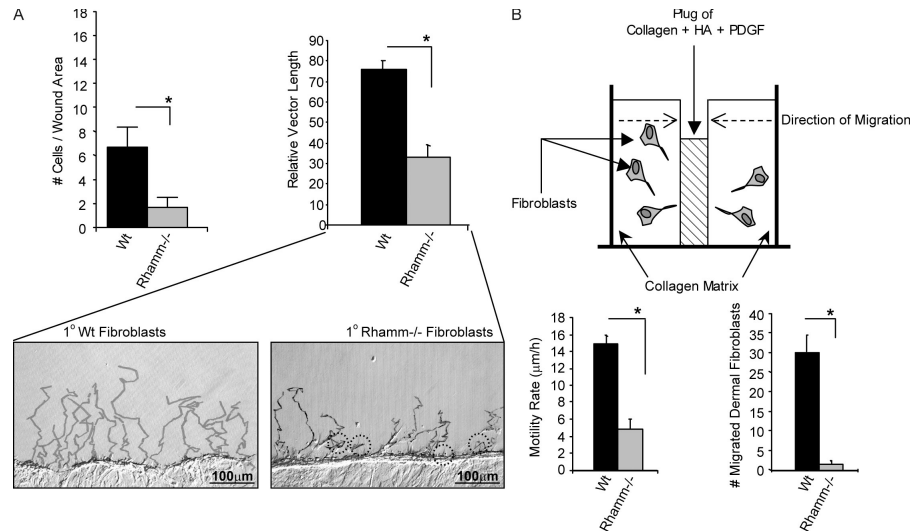
at the cell surface and regulate multiple functions by transmitting signals across the cell membrane. Examples include epimorphin/syntaxin-2 and autocrine motility factor/phosphoglucose isomerase (Radisky et al., 2003; Nickel, 2005). However, neither the physiological functions of proteins such as Rhamm nor the mechanisms by which these proteins regulate signaling pathways are known.

We isolated cell surface Rhamm as a motogenic factor required for rapid fibroblast motility, and we and others also provided evidence for a role of both cell surface and intracellular Rhamm in G$_2$M progression in culture (Turley et al., 2002; Adamia et al., 2005). We showed that Rhamm expression is high in aggressive human fibromatoses (desmoid) tumors (Tolg et al., 2003) and demonstrated that genetic deletion of Rhamm strongly reduced desmoid tumor initiation and invasion in a mutant adenomatous polyposis coli and β-catenin–driven mouse model of this mesenchymal tumor. Fibroproliferative processes such as aggressive fibromatosis resemble proliferative/migratory stages of wound healing (Cheon et al., 2002). The expression of Rhamm is modulated during wounding (Lovvorn et al., 1998) and by fibrogenic cytokines such as TGF-β (Samuel et al., 1993). Because factors that regulate fibroblast function play dual roles in wound repair and tumorigenesis (Park et al., 2000; Bissell and Radisky, 2001), we have assessed whether Rhamm is involved in response to injury using models of "wounds" with Rhamm$^{-/-}$ (Rh$^{-/-}$) fibroblasts in vitro as well as excisional skin wounds in vivo with Rh$^{-/-}$ mice. We show that Rhamm loss results in defective migration in culture as a result of aberrant CD44–ERK1,2 (extracellular-regulated kinase 1,2) signaling. We also show that ERK1,2 activity is defective in early phases of skin repair in Rh$^{-/-}$ mice and that this defect is associated with aberrant mesenchymal cell migration and differentiation.

Results

Fibroblast migration and invasion in culture requires Rhamm and ERK1,2

We and others have previously shown that Rhamm mediates cell migration on tissue culture plastic (Turley et al., 2002).

To determine whether Rhamm is required for fibroblast migration under more physiological settings and whether other proteins compensate for loss of Rhamm expression, the motogenic behavior of Rh$^{-/-}$ and wild-type (Wt) fibroblasts were compared using scratch wounds and 3D collagen gel assays, which are designed to mimic aspects of migration in vivo (Reid et al., 2004). Significantly fewer Rh$^{-/-}$ than Wt fibroblasts migrated across 3-mm scratch wounds in culture (Fig. 1 A). Time lapse of wounds revealed that motility speed of Rh$^{-/-}$ fibroblasts was less than Wt (Fig. 1 A). To confirm that Rhamm expression is sufficient to restore migration to Wt levels, we expressed full-length Rhamm (Rh^{FL}) cDNA in Rh$^{-/-}$ fibroblasts. This rescued migration defects (Fig. S1 a, available at http://www.jcb.org/cgi/content/full/jcb.200511027/DC1). Thus, loss of Rhamm expression results in an inherent migration defect related to a reduced ability of fibroblasts to orient and locomote toward haptotactic cues rapidly.

The invasive properties of Rh$^{-/-}$ versus Wt fibroblasts were compared in 3D collagen type I gels (Fig. 1 B). Migration of primary Rh$^{-/-}$ dermal fibroblasts into the PDGF/HA/collagen gel plug was reduced by 90% compared with Wt fibroblasts (Fig. 1 B), indicating an intrinsic defect in haptotaxis and invasion of Rh$^{-/-}$ fibroblasts. Rh^{FL} expression rescued these defects (Fig. S1 b).

We previously showed that Rhamm is required for activation of ERK1,2 in culture (Zhang et al., 1998). Fibroblast migration requires appropriate temporal regulation of signaling pathways such as ERK1,2, which provide cues for promoting and sustaining migration/invasion (Krueger et al., 2001). To determine whether ERK1,2 activity and/or subcellular targeting is aberrant in Rh$^{-/-}$ fibroblasts and whether the loss of Rhamm is the direct cause of these defects, we quantified serum induction of ERK1,2 activity in Rh$^{-/-}$ versus Rh^{FL}-rescued Rh$^{-/-}$ fibroblasts using ELISA, Western blots, and confocal microscopy (Fig. 2). ELISA analysis showed activation of ERK1,2 in both Rh^{FL}-rescued and Rh$^{-/-}$ fibroblasts (Fig. 2 A), but activity was less and declined more rapidly in Rh$^{-/-}$ cells (Fig. 2 A). Western blots confirmed these results (Fig. 2 B). Confocal analysis showed that active ERK1,2 are targeted to
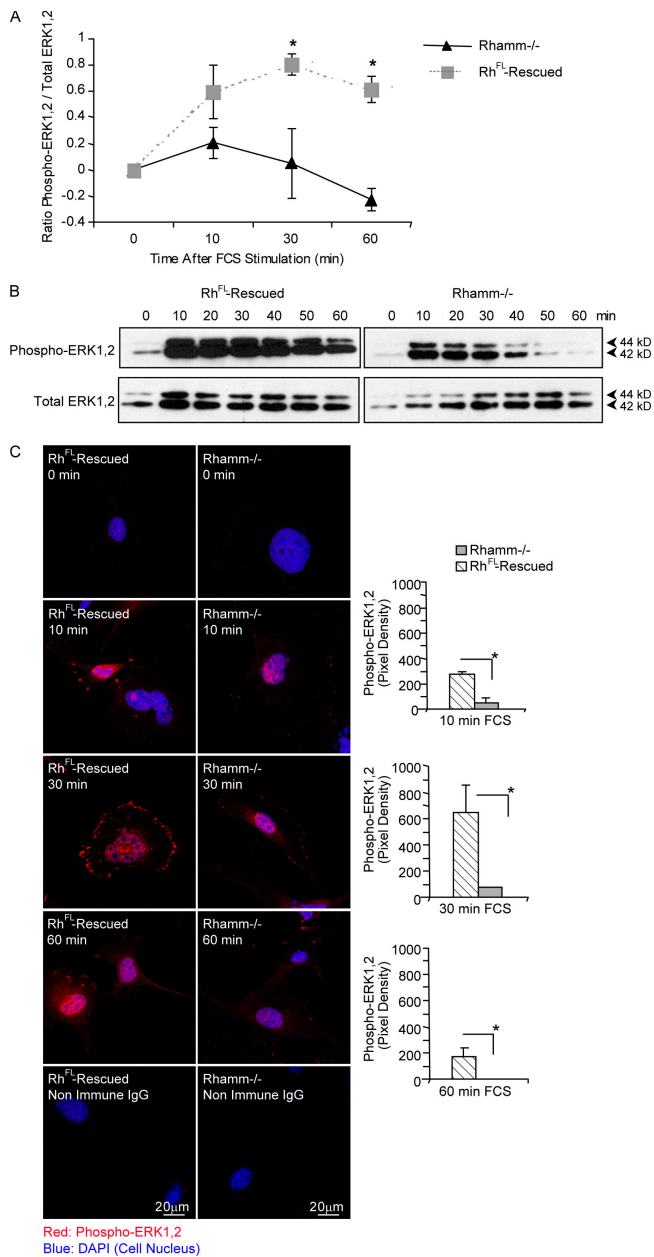
Figure 2. Serum-induced ERK1,2 activation is defective in Rhamm$^{-/-}$ fibroblasts. (A) ELISA of total cellular phospho-ERK1,2. Active ERK1,2 levels are significantly higher after serum stimulation in Rh^{FL}-rescued than in Rh$^{-/-}$ fibroblasts. Values at 0 min were subtracted from values at 30 and 60 min. Mean and SEM; $n = 3$ replicates. One of three experiments is shown. (B) Western blots of phospho-ERK1,2. Rh^{FL}-rescued fibroblasts sustain serum-induced ERK1,2 activity for 50 min compared with 10 min in Rh$^{-/-}$ fibroblasts. One of five experiments is shown. (C) Confocal micrographs and image analysis of phospho-ERK1,2. Overall levels and nuclear (blue) targeting of phospho-ERK1,2 (red) are reduced in Rh$^{-/-}$ compared with Rh^{FL}-rescued fibroblasts. Mean and SEM; $n = 15$ cells for each time point. One of four experiments is shown. *, $P < 0.05$.

the nucleus in both Rh^{FL}-rescued and Rh$^{-/-}$ fibroblasts, but activity was significantly less in Rh$^{-/-}$ cells (Fig. 2 C). A similar reduction in activated ERK1,2 was observed in other subcellular compartments of Rh$^{-/-}$ cells, including lamellae. These results suggest that Rhamm is required for sustaining ERK1,2 activity in multiple subcellular compartments, a process that

can affect fibroblast motility and differentiation (Hornberg et al., 2005).

Rhamm, CD44, and ERK1,2 form complexes required for activating ERK1,2

CD44 is a commonly expressed, integral membrane adhesion and HA receptor that activates motogenic signaling cascades, including ERK1,2 (Bourguignon et al., 2002). CD44 coassociates with ERK1,2 via adaptor proteins that bind to its cytoplasmic tail (Bourguignon et al., 2005; Marhaba et al., 2005). To begin to identify molecular mechanisms that are deficient in Rh$^{-/-}$ fibroblasts, we first assessed whether Rhamm can coassociate with CD44 and whether both Rhamm and CD44 are required for activation of ERK1,2. CD44s protein was expressed in equivalent amounts in Rhamm-expressing and Rh$^{-/-}$ fibroblasts (Fig. 3 A). The ability of Rhamm, CD44, and ERK1,2 to associate with each other in Rh^{FL}-rescued fibroblasts was demonstrated in pull-down assays (Fig. 3 B). Confocal analyses confirmed coassociation of these proteins in cell processes and CD44-positive perinuclear vesicles (Fig. 3). Both anti-CD44 and anti-Rhamm antibody significantly reduced the intensity of nuclear phospho-ERK1,2 (Fig. 4, A and B), raising the possibility that CD44–Rhamm complexes are required for maximal activation of ERK1,2. To test this, the consequences of blocking Rhamm, CD44, and ERK1,2 motogenic functions on fibroblast migration were measured.

Rhamm, CD44, and ERK1,2 are required for motility in response to serum and HA
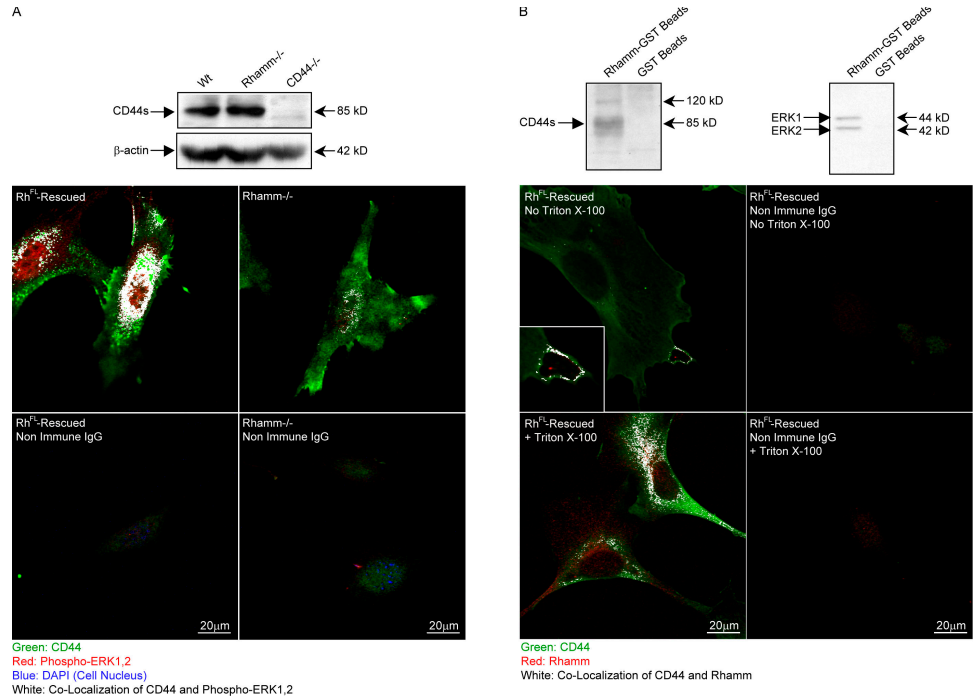
Anti-Rhamm, anti-CD44 antibody, and a mitogen-activated kinase kinase 1 (Mek1) inhibitor (UO126) significantly blocked serum-induced motility of Rh^{FL}-rescued but not Rh$^{-/-}$ fibroblasts (Fig. 4, C and D), confirming that Rhamm, CD44, and ERK1,2 activity are required for optimal motility.

Signaling through CD44 and ERK1,2 are required for motility in response to HA (Bourguignon et al., 2005). We therefore next measured the motility of Rh^{FL}-rescued versus Rh$^{-/-}$ fibroblasts stimulated with HA. To render nontransformed cells sensitive to HA, fibroblasts can be pretreated with PMA; this activates PKC-dependent processes, permitting motogenic responses to HA (Hall et al., 2001). Compared with PMA treatment alone, a mixture of high molecular weight HA and oligosaccharides significantly promoted random motility of Rh^{FL}-rescued but not Rh$^{-/-}$ fibroblasts (Fig. 4 D). Motogenic stimulation by HA required cell surface Rhamm, as anti-Rhamm antibodies blocked a response to HA. The inability of HA to increase Rh$^{-/-}$ fibroblast motility was puzzling because these cells express similar levels of CD44s as Wt (Fig. 3 A). We suspected that the localization of CD44 to the cell surface might be altered in Rh$^{-/-}$ cells, as a reduced number of perinuclear CD44-positive vesicles, which can traffic to the cell surface (Robertson et al., 2006), were observed in Rh$^{-/-}$ versus Rh^{FL}-rescued fibroblasts (Fig. 3 A).

Rhamm promotes surface display of CD44 and codistribution of CD44 with ERK1,2

Adherent Rh$^{-/-}$ fibroblasts exhibited reduced CD44 surface display compared with Rh^{FL}-rescued fibroblasts (Fig. 5 A). Both

Figure 3. **CD44 coassociates with Rhamm and active ERK1,2.** (A) CD44 protein expression and distribution. Rh$^{-/-}$ and Wt fibroblasts express similar levels of CD44 proteins (β-actin loading control). One of three experiments is shown. Confocal analysis shows that CD44 (green) occurs mainly in vesicles with phospho-ERK1,2 (red; colocalization shown as white) after Rh^{FL} rescue. CD44 staining is amorphous and not associated with phospho-ERK1,2 in Rh$^{-/-}$ fibroblasts. One of four experiments is shown. (B) Rhamm, CD44, and ERK1,2 form complexes. Recombinant Rhamm-GST protein–Sepharose (Rhamm-GST beads) pulls down CD44s, a possible CD44 variant (120 kD), and ERK1,2. One of three experiments is shown. Confocal analysis confirms that Rhamm (red) and CD44 (green) colocalize (white) in processes of Rh^{FL}-rescued fibroblasts (no Triton X-100) and in vesicles (+Triton X-100). One of three experiments is shown.

Green: CD44
Red: Phospho-ERK1,2
Blue: DAPI (Cell Nucleus)
White: Co-Localization of CD44 and Phospho-ERK1,2

Green: CD44
Red: Rhamm
White: Co-Localization of CD44 and Rhamm

Mek1 inhibition with UO126 (Fig. 5 A) and anti-Rhamm antibody (Fig. 5 A) reduced CD44 display. Rh^{FL}-rescued fibroblasts also showed increased colocalization of CD44 with active ERK1,2, particularly in the cell nucleus and perinuclear vesicles, compared with Rh$^{-/-}$ fibroblasts (Fig. 5 B). Anti-Rhamm antibody reduced colocalization of these proteins (Fig. 5 B). These results suggest a role for cell surface Rhamm in ERK1,2 activation and, consequently, surface display of CD44. We next examined whether activation of ERK1,2 in the absence of Rhamm would have a similar effect.

Expression of activated Mek1 or restoration of cell surface Rhamm rescues Rh$^{-/-}$ fibroblast defects

Expression of active Mek1 restored sustained serum-induced ERK1,2 activity in Rh$^{-/-}$ fibroblasts (Fig. 6, A and B). This effect was not enhanced by coexpression of Rh^{FL} (Fig. 6 A). Mek1 also restored migration of Rh$^{-/-}$ fibroblasts (Fig. 6 C) and promoted CD44 display (Fig. 6 C). These results suggest that Rhamm and Mek1/ERK1,2 act on the same CD44-regulated motogenic signaling pathway because Mek1 can compensate

Figure 4. **Cell surface Rhamm (CD168) and CD44 are required for ERK1,2 activity and motility in response to FCS and HA.** (A) Role of cell surface Rhamm in nuclear ERK1,2 activity. Rhamm antibody significantly reduces levels of serum-induced nuclear phospho-ERK1,2. Mean and SEM; $n = 25$ cells. One of four experiments is shown. (B) Role of CD44 in nuclear ERK1,2 activity. CD44 antibody significantly reduces the levels of serum-induced nuclear phospho-ERK1,2. Mean and SEM; $n = 25$ cells. One of four experiments is shown. (C) Motility in response to FCS. Rh^{FL} expression in Rh$^{-/-}$ fibroblasts significantly increases motility. The dotted line is Rh$^{-/-}$ fibroblast motility, which did not vary with treatment. Rh^{FL} rescue requires surface CD44 and ERK1,2 activity, as CD44 antibody or a Mek1 inhibitor (UO126) significantly reduces motility. Rhamm antibody blocks Rh^{FL}-rescued but not Rh$^{-/-}$ fibroblast motility. Mean and SEM; $n = 30$ cells. One of six experiments is shown. (D) Motility in response to HA. Wt, but not Rh$^{-/-}$, fibroblasts increase random motility in response to HA. Rhamm antibody reduces HA-mediated motility of Wt but not Rh$^{-/-}$ fibroblasts. Fibroblasts were first exposed to PMA to generate responsiveness to HA. Mean and SEM; $n = 30$ cells. One of four experiments is shown. *, $P < 0.05$.
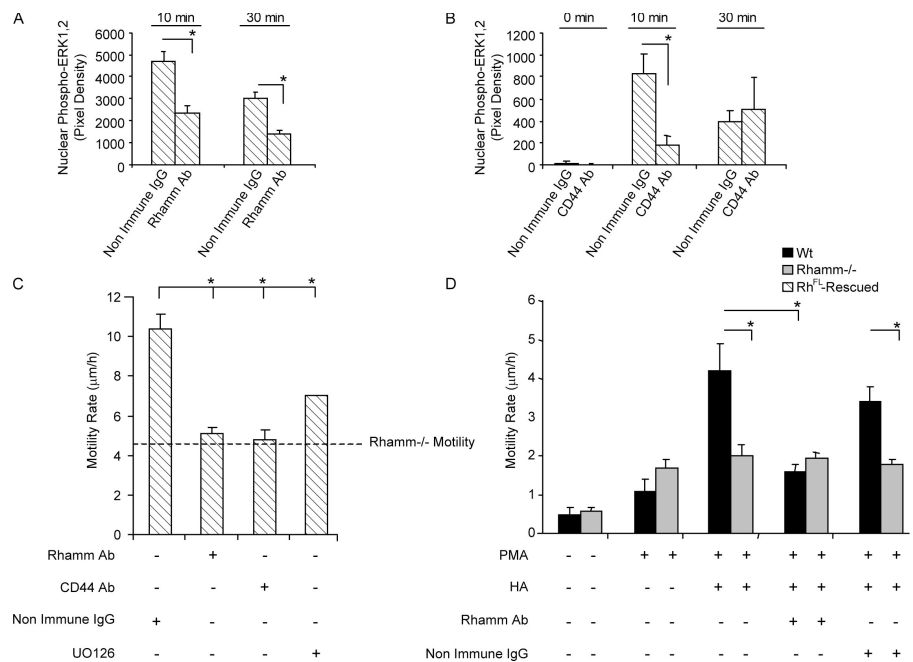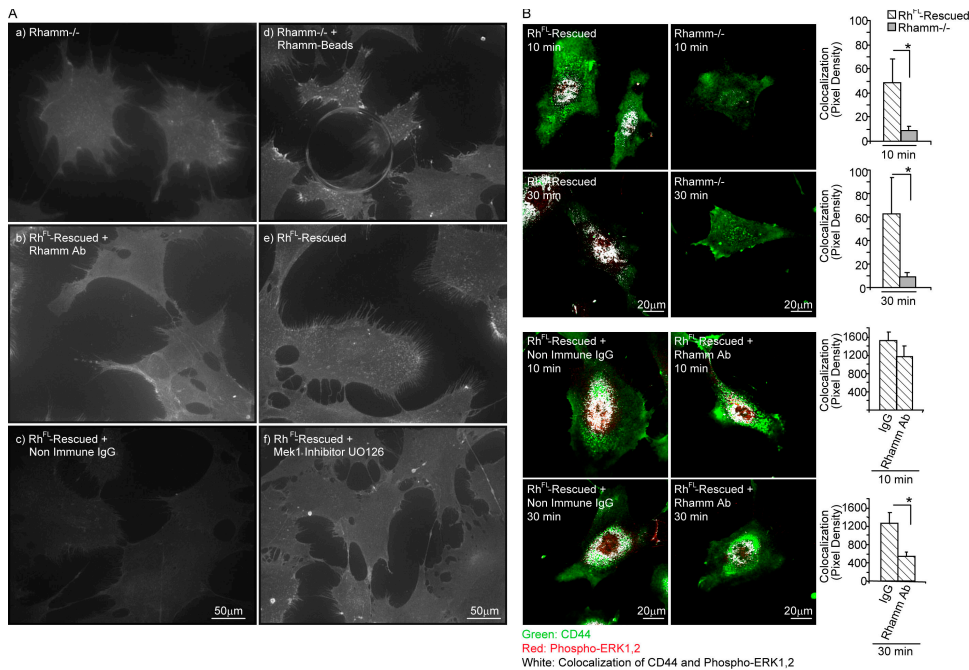
Figure 5. Cell surface Rhamm is required for CD44 display and complexing with phospho-ERK1,2. (A) Effect of Rhamm and ERK1,2 activity on surface display of CD44. (a and d) $Rh^{-/-}$ fibroblasts; (b–f) Rh^{FL}-rescued fibroblasts. Live-cell immunofluorescence shows that $Rh^{-/-}$ fibroblasts exhibit less surface CD44 than Rh^{FL}-rescued fibroblasts. A Mek1 inhibitor and Rhamm antibody block CD44 cell surface display. Recombinant Rhamm beads rescue display on $Rh^{-/-}$ cells in contact with or close to beads. One of three experiments is shown. (B) Effect of Rhamm on CD44 and phospho-ERK1,2 colocalization. Confocal micrographs and image analysis show that serum stimulates greater colocalization (white) of CD44 (green) and phospho-ERK1,2 (red) in Rh^{FL}-rescued than $Rh^{-/-}$ fibroblasts, and colocalization is reduced by Rhamm antibody. Mean and SEM; n = 25 cells. One of four experiments is shown. *, $P < 0.05$.

for Rhamm in these functions. Both cell surface and intracellular Rhamm have been proposed to regulate functions associated with motility and to affect signaling cascades (Turley et al., 2002; Adamia et al., 2005). The ability of anti-Rhamm antibody to mimic defective motogenic signaling of $Rh^{-/-}$ fibroblasts suggests a role for cell surface Rhamm in these functions but does not exclude an involvement of intracellular Rhamm. Blocking antibodies do not permit a direct assessment of the relative roles of cell surface versus intracellular Rhamm in cell functions. To directly assess the importance of cell surface Rhamm to motogenic signaling, we exposed $Rh^{-/-}$ fibroblasts to recombinant Rhamm linked to Sepharose beads to restrict it to the extracellular compartment.

Rhamm beads significantly stimulated motility of $Rh^{-/-}$ fibroblasts that contacted beads, whereas GST beads had no effect (Fig. 7 A). Both anti-CD44 and anti-Rhamm antibody (unpublished data) significantly blocked Rhamm bead–stimulated motility. CD44 surface display was dramatically increased in $Rh^{-/-}$ fibroblasts contacting Rhamm beads (Fig. 5 A). Importantly, fibroblasts deficient in both Rhamm and CD44 ($Rh^{-/-}$: $CD44^{-/-}$) did not increase motility in response to Rhamm beads (Fig. 7 A). Collectively, these results indicate that cell surface Rhamm is required for CD44 display and motility but that intracellular Rhamm proteins are not required for these functions. Furthermore, these results show that CD44 is required for the motogenic effect of cell surface Rhamm.

To understand the molecular mechanisms by which cell surface Rhamm promotes CD44 surface display and increased motility, we determined whether Rhamm bead–induced motility of $Rh^{-/-}$ fibroblasts requires ERK1,2 activity. Inhibition of Mek1 significantly reduced motility of $Rh^{-/-}$ fibroblasts in contact with Rhamm beads (Fig. 7 A). Conversely, Rhamm beads significantly stimulated serum-induced ERK1,2 activity and translocation to the nucleus (Fig. 7 B). ERK1,2 activity was

not as high as that of Rh^{FL}-rescued fibroblasts, suggesting a possible role for intracellular Rhamm forms in maintaining maximal activity of these kinases. A role for CD44 in Rhamm bead–promoted ERK1,2 activity was shown by the ability of CD44 antibodies to block Rhamm bead effects and by the lack of Rhamm bead–induced ERK1,2 activity in $Rh^{-/-}$:$CD44^{-/-}$ fibroblasts. Because expression of Rhamm and CD44 are increased during excisional skin wound repair (Lovvorn et al., 1998) and fibroblast migration and differentiation are essential components of successful excisional wound repair, we asked whether Rhamm loss alters repair of excisional skin wounds in vivo.

Rhamm expression is required to sustain ERK1,2 activity during granulation tissue formation in vivo

We have shown that $Rh^{-/-}$ fibroblasts exhibit defective activation and subcellular targeting of ERK1,2 via CD44. To prove that Rhamm is indeed a player in the physiological regulation of ERK1,2, their activity was quantified in fibroblasts of $Rh^{-/-}$ versus Wt wound granulation tissue. Wt granulation tissue fibroblasts exhibited strong staining for active ERK1,2 3 d after wounding (Fig. 8). Staining intensity increased sixfold by day 7 and did not drop significantly until day 13. $Rh^{-/-}$ granulation tissue fibroblasts also exhibited strong activation of ERK1,2 at 3 d after wounding but dropped dramatically by day 7 and remained low at day 13 (Fig. 8). These differences in $Rh^{-/-}$ versus Wt ERK1,2 activity were not due to decreases in total ERK1,2 protein levels because immunoblot analyses revealed that $Rh^{-/-}$ and Wt granulation tissue expressed similar amounts of ERK1,2 protein (unpublished data). These results suggest that Rhamm expression is required for sustaining ERK1,2 activity in granulation tissue fibroblasts in vivo as well as in culture.
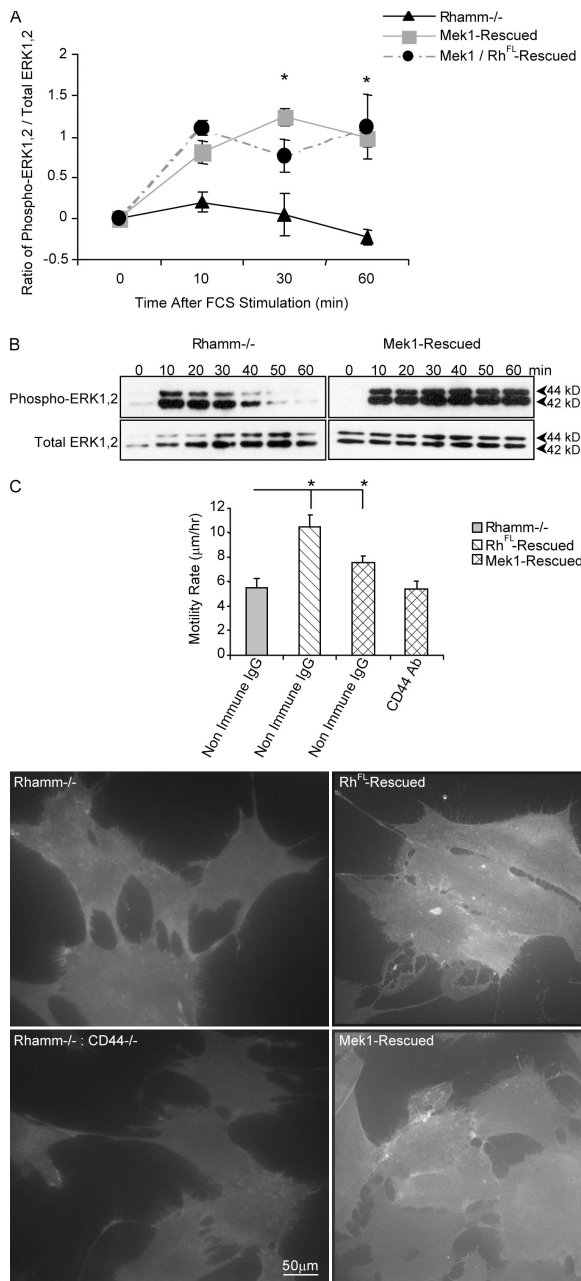
Figure 6. **Mutant active Mek1 rescues ERK1,2 activity, motility, and CD44 surface display in Rh$^{-/-}$ fibroblasts.** (A) ELISA of active ERK1,2. Expression of Mek1 in Rh$^{-/-}$ fibroblasts restores serum-induced ERK1,2 activity. Values at 0 min were subtracted from values at 30 and 60 min. Mean and SEM; $n = 3$ replicates from one of three experiments. (B) Western blot of active ERK1,2. Western blots confirm rescue of ERK1,2 activity by Mek1 in Rh$^{-/-}$ fibroblasts. One of five experiments is shown. (C) Motility and cell surface CD44 display. Expression of Mek1 in Rh$^{-/-}$ fibroblasts significantly increases motility, which is blocked by anti-CD44 antibody. Mean and SEM; $n = 30$ cells from one of three experiments. Live-cell immunofluorescence shows that Mek1 expression restores surface CD44 display in Rh$^{-/-}$ fibroblasts. The specificity of the anti-CD44 antibody is demonstrated by a lack of fluorescence in murine CD44$^{-/-}$:Rh$^{-/-}$ fibroblasts. One of three experiments is shown. *, $P < 0.05$.

MAPKs have been implicated in processes relevant to wound repair, including contraction, cell migration, and mesenchymal differentiation (Bost et al., 2005; Hornberg et al., 2005). We therefore next examined the consequences of

Rhamm loss and aberrant ERK1,2 signaling on wound repair in vivo.

Loss of Rhamm expression results in abnormal granulation tissue formation and resolution in skin wounds

We first confirmed that Rhamm expression increases during repair of excisional wounds by analyzing wound Rhamm mRNA during the first 7 d after injury. RT-PCR analysis of uninjured skin confirmed low Rhamm expression (Fig. S2 a, available at http://www.jcb.org/cgi/content/full/jcb.200511027/DC1). A marked increase in Rhamm mRNA was obvious 1 d after injury, and expression was increased until day 3, when mRNA levels began to drop. By day 7, the mRNA levels were only slightly higher than those observed in uninjured skin. These results indicate that Rhamm is expressed during wound contraction, reepithelialization, and early granulation tissue formation. The consequence of Rhamm loss for the integrity of these early processes was recorded.

Wt and Rh$^{-/-}$ wounds both contracted by 1–3 d after injury, but early contraction of Rh$^{-/-}$ wounds was significantly reduced compared with Wt (Fig. S2 b). By day 14, Wt and Rh$^{-/-}$ wounds appeared resolved at the macroscopic level (unpublished data). However, analysis of serial tissue sections of wound centers revealed significant reductions in contraction and obvious differences in the dermal structure of Rh$^{-/-}$ wounds at all time points (Fig. S2 c). 21 d after injury, both the thickness and the cellularity of the remodeling dermis were significantly greater in Rh$^{-/-}$ versus Wt wounds. In addition, the differentiation of structures such as hair shafts and muscle within the wound site was reduced in Rh$^{-/-}$ versus Wt wounds (Fig. S3 b, available at http://www.jcb.org/content/full/jcb.200511027/DC1). A significant decrease in the thickness of Rh$^{-/-}$ versus Wt dermis was also observed before injury (Fig. S3 a). These observations are consistent with an ERK1,2-regulated defect in Rh$^{-/-}$ wound fibroblast function. We next analyzed the consequences of Rhamm loss on granulation tissue formation/resolution, a process that is dependent on fibroblasts.

A temporal defect in the formation and resolution of granulation tissue was confirmed in Rh$^{-/-}$ versus Wt wounds (Fig. 9). Tenascin-positive granulation tissue was abundant in day 3 Wt wounds and began to decrease by day 7 (Fig. 9 A). At day 14, Wt wound granulation tissue was largely resolved (Fig. 9 A). In contrast, the area of tenascin-positive granulation tissue in day 3 and 7 Rh$^{-/-}$ wounds was smaller than Wt. Rh$^{-/-}$ day 14 wounds were still strongly tenascin-positive and highly variable (Fig. 9 B), as the pattern of staining was "patchy," in contrast to Wt (Fig. 9 A). An additional difference in Rh$^{-/-}$ wounds was the transient appearance of a thick layer of subcutaneous adipocytes in day 1–3 Rh$^{-/-}$ wounds (Fig. 10 A; unpublished data). These results suggest that a prominent effect of Rhamm loss during wound repair may be a miscuing of signals required for a correct ratio of fibroblasts to adipocytes that arise from progenitor cells, which leads to aberrant regulation of granulation tissue formation and resolution.

Fibroplasia is a particularly prominent feature of granulation tissue in excisional skin wounds. The biological
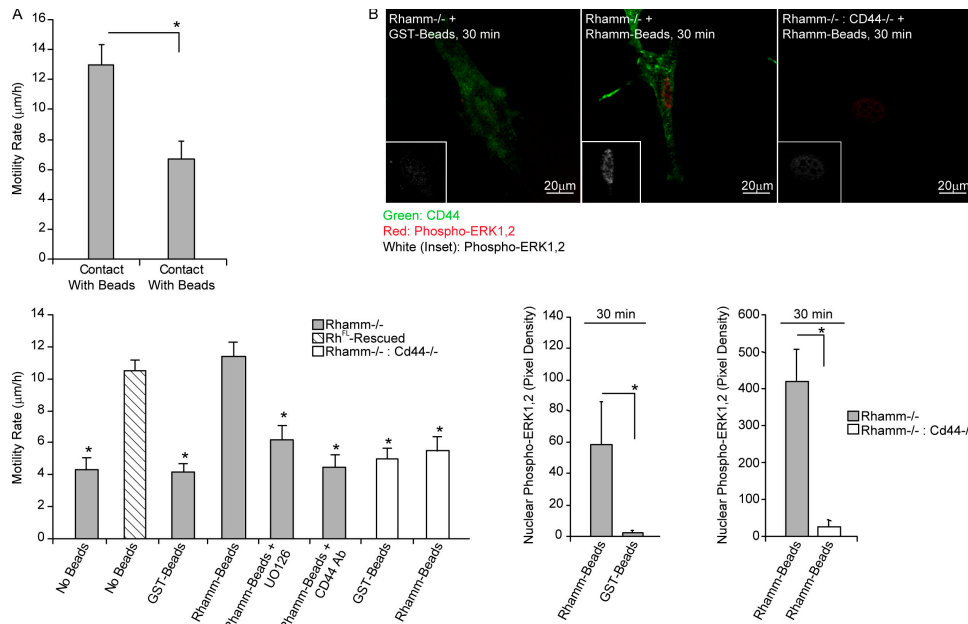
Figure 7. **Cell surface Rhamm rescues motility of Rhamm$^{-/-}$ fibroblasts.** (A) Motility in response to Rhamm beads. Rh$^{-/-}$ fibroblast motility is significantly increased when cells contact recombinant Rhamm beads, compared with control GST beads. Rhamm bead–stimulated motility is similar to Rh^{FL}-rescued fibroblast motility and is blocked by a Mek1 inhibitor and CD44 antibody. Mean and SEM; $n = 30$ cells. One of eight experiments is shown. (B) ERK1,2 activation in response to Rhamm beads. Serum-induced ERK1,2 activity (red; white in insets) in Rh$^{-/-}$ fibroblasts is significantly stimulated by Rhamm beads but not control GST beads. ERK1,2 activity is not increased in Rh$^{-/-}$ fibroblasts when CD44 (green) is not expressed (Rh$^{-/-}$:CD44$^{-/-}$). Rhamm beads do not increase nuclear phospho-ERK1,2 in Rh$^{-/-}$:CD44$^{-/-}$ fibroblasts. Mean and SEM; $n = 25$ cells. One of three experiments is shown. *, $P < 0.05$.

activities of fibroblasts are key factors in the formation of early granulation tissue architecture (Reid et al., 2004). Robust fibroplasia, as quantified by the density/unit area of granulation tissue fibroblasts, was apparent in Wt wounds on day 3 and was increased by day 7 (Fig. 10 A). Myofibroblasts, detected by smooth muscle actin staining, appeared in Wt wounds by day 7 (Fig. 10 B). Fibroplasia was observed in day 3 and 7 Rh$^{-/-}$ granulation tissue but was blunted and accompanied by a significant decrease in myofibroblasts at day 7 (Fig. 10, A and B). The presence of abundant wound-edge adipocytes, indicated by the presence of vacuolated cells (Fig. 10 A, arrow), was confirmed by staining with the lipophylic dye BODIPY493/503 (Gocze and Freeman, 1994; unpublished data). Rh$^{-/-}$ cells explanted from both uninjured skin (day 0) and day 7 wounds expressed less smooth muscle actin and accumulated more lipid than explanted Wt cells (Fig. 10 C). Thus, deletion of Rhamm results in lower fibroblast density as well as aberrant differentiation in Rh$^{-/-}$ granulation tissue in vivo and in culture.

Discussion

Our study identifies Rhamm as a fibrogenic factor that is required for temporal and spatial regulation of granulation tissue formation and resolution. An underlying signaling defect associated with Rh$^{-/-}$ wounds is deregulated ERK1,2 activation, which promotes fibroblast migration as well as mesenchymal cell differentiation. This conclusion is supported by the demonstration that Rh$^{-/-}$ fibroblasts are unable to appropriately activate ERK1,2 in culture and exhibit migration defects as measured by several locomotion assays, and that these defects are rescued by expression of mutant active Mek1. Our results further reveal an autocrine mechanism by which cell surface Rhamm promotes motility in culture. This form of Rhamm promotes ERK1,2 activation via an association with

CD44, which in turn is required for maintaining cell surface display of CD44. ERK1,2 is acting "downstream" of cell surface Rhamm in this function, as expression of mutant active Mek1 is sufficient to maintain cell surface CD44, activate ERK1,2, and restore motility in the absence of Rhamm expression. This motogenic mechanism involves formation of cell surface Rhamm–CD44–ERK1,2 complexes and is apparently required for both growth factor– and HA-mediated motility. These findings identify for the first time a mechanism by which Rhamm, a nonintegral membrane protein, can activate intracellular signaling cascades and provide a novel mechanism by which ERK1,2 promotes motility. Furthermore, our results suggest a previously unidentified role for ERK1,2 activation kinetics in excisional skin wound granulation tissue formation/resolution.

Rhamm belongs to a group of proteins that are predominantly intracellular but can be exported to the cell surface via unconventional transport mechanisms that do not involve the export through the Golgi/ER (Nickel, 2005). We show that cell surface Rhamm is displayed in culture after injury, and our results have begun to clarify functions for cell surface Rhamm versus intracellular Rhamm forms. Although we did not set out to define a role for intracellular Rhamm, indirect evidence suggests that it plays a role in mitotic events, at least in culture, as cell surface Rhamm did not rescue the abnormal mitosis observed during time-lapse analysis of Rh$^{-/-}$ fibroblasts (unpublished data). These results are consistent with evidence for intracellular Rhamm function during progression through G$_2$M of the cell cycle (Mohapatra et al., 1996; Maxwell et al., 2003, 2005) and its presence on centrosomes and mitotic spindle microtubules (Maxwell et al., 2003; Evanko et al., 2004). Nevertheless, our current data do not provide support for an essential role of either intracellular or cell surface Rhamm in mitotic spindle formation and cell cycle regulation during wound repair in dermal fibroblasts in vivo, as judged by the lack of detectable
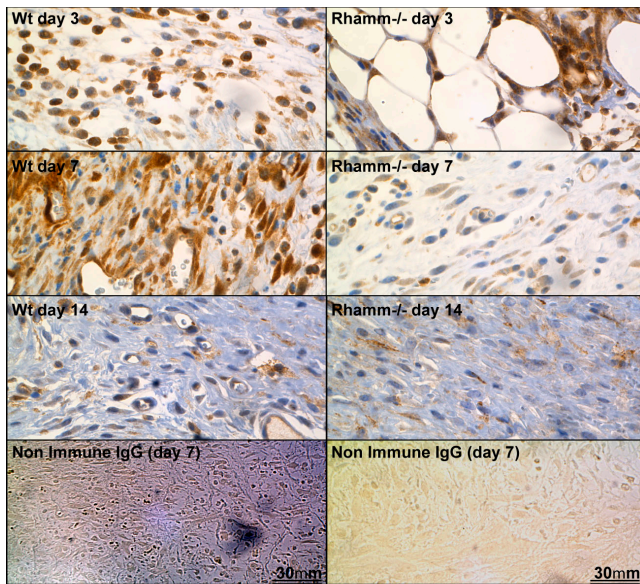
Brown Staining: Phospho-ERK1,2
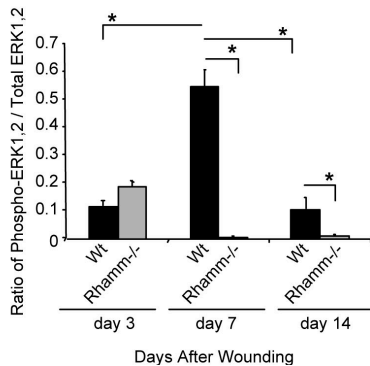Blue Staining: Hematoxylin (Cell Nuclei)

Figure 8. **ERK1,2 activation is aberrant in Rhamm$^{-/-}$ wound granulation tissue.** Both Wt and Rh$^{-/-}$ granulation tissue fibroblasts are positive for phospho-ERK1,2 on day 3 after wounding (brown). ERK1,2 activity significantly increases in Wt wound granulation tissue by day 7 and drops to background by day 14. ERK1,2 activity prematurely drops in Rh$^{-/-}$ wound granulation tissue to background at day 7 and remains low at day 14. Mean and SEM; $n = 15$ images of three serial sections of wounds from five Wt and Rh$^{-/-}$ mice. *, $P < 0.05$.

control cell motility, invasion, and cytoskeleton remodeling during migration in culture (Yao et al., 2003; Bost et al., 2005). Our results show that migration defects of Rh$^{-/-}$ fibroblasts result from an inability to sustain and maximally activate ERK1,2 after growth factor stimulation. These results are consistent with our previous evidence that cell surface Rhamm is required for PDGF-stimulated ERK1,2 activity in mesenchymal cells and for promoting migration by regulating signaling through upstream activators of ERK1,2, including HA, Src, Ras, and FAK (Hall et al., 1995, 1996; Turley et al., 2002). Others have also documented a role for cell surface Rhamm in activating signaling cascades that regulate motility and that directly or indirectly affect ERK1,2 activation (Lokeshwar and Selzer, 2000; Aitken and Bagli, 2001; Goueffic et al., 2006). Although cell surface Rhamm can promote ERK1,2 activity to levels sufficient to sustain motility in the absence of intracellular forms, levels were lower than in cells expressing both cell surface and intracellular Rhamm (e.g., Rh^{FL}-rescued fibroblasts). Furthermore, although cell surface Rhamm–activated ERK1,2 translocated to the nucleus, activity did not persist here as it did when intracellular Rhamm was also present. These results indirectly implicate intracellular Rhamm forms in aspects of ERK1,2 activation/compartmentalization. These intracellular deficiencies did not affect the ability of cell surface Rhamm to promote motility during our experimental time frame but could affect other functions associated with ERK1,2 activity, such as invasion and mitosis, neither of which were rescued by cell surface Rhamm alone (unpublished data). The consequences of ERK1,2 signaling on cell differentiation, migration, and proliferation depends on activation kinetics and subcellular compartmentalization (Colucci-D'Amato et al., 2003; Hendriks et al., 2005; Hornberg et al., 2005). These factors are determined by receptor dimerization and internalization, cross talk with other receptors, association of ERK1,2 with adaptors, and activation of other kinases or phosphatases that modify ERK1,2 activity. Our study raises the possibility that cell surface and intracellular Rhamm may differentially affect the activation levels and subcellular targeting of ERK1,2, which have consequences to motility- and invasion-related gene expression and phosphorylation of intracellular substrates that are involved in cell migration/invasion (Huang et al., 2004).

ERK1,2 regulate motility by both transcriptional and post-translational mechanisms. For example, initiation and early phases of migration during wound repair do not require transcription (Providence and Higgins, 2004) but, rather, involve phosphorylation of predominantly cytoskeleton-associated substrates required for motility, such as myosin (Huang et al., 2004; Helfman and Pawlak, 2005; Simoes and Fierro, 2005). Our results also identify a role for ERK1,2 activity in sustaining cell surface display of CD44, an integral membrane protein required for motility in response to growth factors and HA (Toole, 2004). ERK1,2 promote recycling of clathrin-negative early endosomes back to the cell surface, a pathway associated with recycling of β1 integrins and E-cadherin (Robertson et al., 2006). A similar ERK1,2-regulated recycling event may be responsible for maintaining CD44 at the cell surface.

We have shown that CD44 and Rhamm have overlapping functions in regulating migration events and that Rhamm can
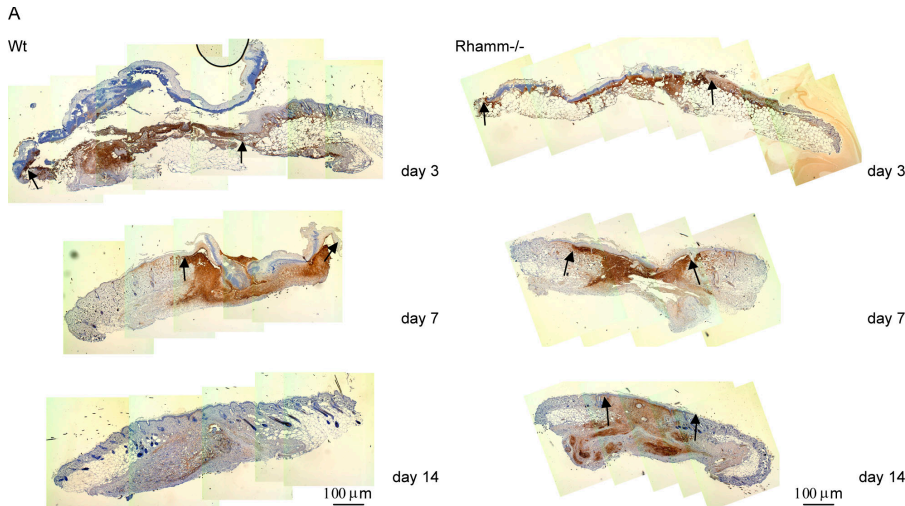
differences in proliferation or apoptotic indices within Rh$^{-/-}$ versus Wt wound sites. The slightly disorganized migration of Rh$^{-/-}$ fibroblasts from scratch wound assays on tissue culture plastic is consistent with a possible centrosome defect that could contribute to aberrant migration (Watanabe et al., 2005) and merits further experimentation. A role for Rhamm in collagen contraction has been controversial in culture (Bagli et al., 1999; Travis et al., 2001). Unexpectedly, therefore, our studies suggest that Rhamm is necessary for recruitment/differentiation of myofibroblasts and contraction of the wound bed. As is increasingly reported and recognized, both of these results emphasize the importance of context and the microenvironment in regulating tissue-specific signaling (Bissell et al., 2003). Thus, data obtained in culture, especially on 2D substrata, need to be confirmed in vivo.

ERK1 and -2 are closely related MAPK isoforms that are activated by Mek1 or -2 and regulate signaling pathways that
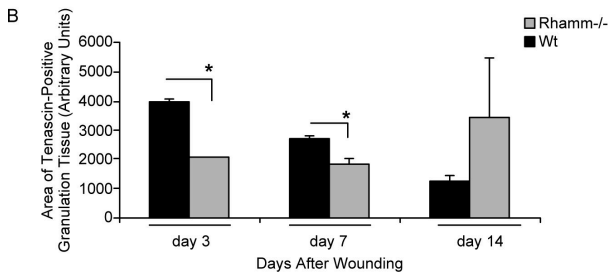
Figure 9. Wound granulation tissue formation/resolution is altered in Rhamm$^{-/-}$ mice. (A) Tenascin protein expression in wound sections. Wound granulation tissue is abundant in day 7 Wt mice (brown) and largely resolved by day 14, as indicated by loss of tenascin staining. In comparison, tenascin-positive Rh$^{-/-}$ granulation tissue area is reduced on days 3 and 7 and "patchy" on day 14, suggesting delayed and abnormal patterning of granulation tissue resolution. (B) Quantification of tenascin-positive granulation tissue. Wt granulation tissue area is significantly greater than Rh$^{-/-}$ at both day 3 and 7 after wounding. Mean and SEM; $n = 3$ serial sections of wound tissue composites from eight Rh$^{-/-}$ and Wt mice. *, $P < 0.05$.

compensate for loss of CD44 in aspects of splenocyte migration into arthritic joints, although the reverse may not be true (Nedvetzki et al., 2004). These and other studies (Turley et al., 1993; Goueffic et al., 2006) suggest that Rhamm can promote cell motility independently of CD44. Very likely, in these instances, cell surface Rhamm associates with other adhesion receptors involved in cell motility, and partnering may depend on expression and cell surface display levels of these receptors, which will vary with the nature of disease, cell type, and temporal stage of wound repair.
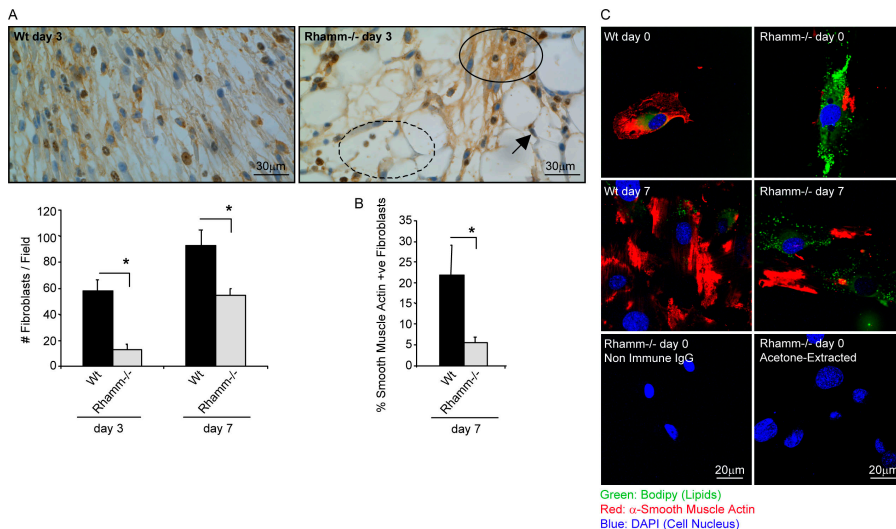

Figure 10. Fibroblast density is reduced and wound granulation tissue cell heterogeneity is increased in Rhamm$^{-/-}$ mice. (A) Fibroblast density in granulation tissue. Granulation tissue fibroblast (elongated, vimentin-positive cells, brown) density is significantly reduced in Rh$^{-/-}$ versus Wt granulation tissue on days 3 and 7 after injury. The arrow indicates a vacuolated cell (adipocyte). Rh$^{-/-}$ fibroblast density is heterogeneous (e.g., dotted circle is sparse; filled line circle is dense) and was averaged per microscope field. Mean and SEM; $n = 4$ serial sections of wounds from eight Wt and Rh$^{-/-}$ mice. (B) Smooth muscle actin–positive granulation tissue fibroblasts. The number of wound myofibroblasts (α-smooth muscle actin–positive cells, brown) is significantly reduced in day 7 Rh$^{-/-}$ versus Wt wounds. Mean and SEM; $n = 4$ serial sections from wounds of eight Rh$^{-/-}$ and Wt mice. *, $P < 0.05$. (C) Smooth muscle actin– and lipid-positive fibroblasts (adipocytes) in wound explants. Smooth muscle actin–positive fibroblasts (red) are reduced, whereas lipid-containing cells (green) are increased in Rh$^{-/-}$ versus Wt wound tissue explants. One of two experiments is shown.

Materials and methods

Reagents

Medical-grade HA prepared from bacterial fermentation (a gift from Skye-Pharma) was free of detectable proteins, DNA, or endotoxins (Filion and Phillips, 2001). The average molecular mass and polydispersity was 276.7 and 1.221 kD, respectively. HA oligosaccharides (average molecular mass 10 kD; a gift from F. Winnik, University of Montreal, Montreal, Canada) were prepared by partial digestion with testicular hyaluronidase and purification by gel filtration. The following primary antibodies were used: ERK1 (immunohistochemistry/Western blot), actin (Western blot), vimentin (immunohistochemistry), α-smooth muscle actin (immunohistochemistry), nonimmune IgG (Santa Cruz Biotechnology, Inc.), Ki67 (immunohistochemistry; DakoCytomation), tenascin (immunohistochemistry; Chemicon), phospho-ERK1,2 (immunohistochemistry/Western blot/immunofluorescence; Cell Signaling), CD44 (Western blot/immunofluorescence/blocking; IM7; BD Biosciences), CD44 (blocking; Hermes-3; a gift from D. Naor, The Hebrew University of Jerusalem, Jerusalem, Israel), Rhamm (immunofluorescence; ProSci), and Rhamm (blocking; Zymed Laboratories). Specificity of Rhamm and CD44 antibodies were determined using Rh$^{-/-}$ and CD44$^{-/-}$ cells, respectively. The following secondary antibodies were used: anti-rabbit Alexa 555 and anti-rat Alexa 433 (Invitrogen), HRP-anti-mouse (Bio-Rad Laboratories), anti-rabbit (BD Biosciences), and anti-rat (Santa Cruz Biotechnology, Inc.). ApopTag peroxidase in situ apoptosis detection kit (Chemicon) was used for quantification of apoptosis, and FACE ERK1/2 ELISA kit (Active Motif) was used to detect phospho-ERK1,2. Other reagents used were as follows: human plasma fibronectin (BD Biosciences), PDGF (PDGF-BB), and PMA (Sigma-Aldrich); 50 μM PD098059 and 10 μM U0126 (BD Biosciences); collagen (Vitrogen100; Cohesion); Matrigel (BD Biosciences); immunofluorescence mounting medium with DAPI (Vecta-shield; Vector Laboratories); Cytoseal (Richard-Allan Scientific); and ABC staining system (Santa Cruz Biotechnology, Inc.). All antibodies and reagents were used according to the manufacturer's instructions unless otherwise stated.

Rh$^{-/-}$ mice, mouse embryonic fibroblasts, and dermal fibroblasts

All animal experiments complied with the University of Western Ontario (London, Canada) animal use committee regulations. Preparation of Rh$^{-/-}$ mice and mouse embryonic fibroblasts (Tolg et al., 2003) and CD44$^{-/-}$ mice (Schmits et al., 1997) have been described. Rhamm and CD44 heterozygous mouse mating generated Rh$^{-/-}$:CD44$^{-/-}$ double-knockout mice. Dermal fibroblasts were isolated from newborn skin explants and granulation tissue cells from wound punch explants (cultured dermal side down).

Cell culture, transfection, and antibody blocking

Cell culture was done as described previously (Zhang et al., 1998; Tolg et al., 2003). 25 ng/ml PDGF, 500 ng/ml–1 mg/ml HA, or 10% serum (FCS) were added to 24-h serum-starved, 50% subconfluent fibroblasts plated on 25 μg/ml fibronectin-coated dishes (Hall et al., 1996; Zhang et al., 1998). For HA responsiveness, cells were pretreated with 5 nM PMA (Hall et al., 2001). For antibody blocking experiments, serum-starved cells were preincubated for 30 min with anti-Rhamm antibody, anti-CD44 antibody, or control IgG (10 μg/ml) before the addition of 10% FCS. Immortalized Rh$^{-/-}$ cells were transfected with murine Rh^{FL} and/or mutant active Mek1 (a gift from N. Ahn, University of Colorado at Boulder, Boulder, CO) using Lipofectamine Plus (Invitrogen) as described previously (Zhang et al., 1998) and were selected in 1–5 mg/ml G418 (Sigma-Aldrich).

Time-lapse analysis

Cells were plated and stimulated with HA or PDGF. For FCS stimulation, fibroblasts were plated onto serum-coated flasks. Cells were filmed as described previously (Zhang et al., 1998; Hall et al., 2001).

In vitro wound and invasion assays

Confluent cell monolayers were starved overnight, scratch wounded (3 mm) with a sized cell scraper, and stimulated with FCS or PDGF for 24–48 h. Monolayers were fixed (3% paraformaldehyde), stained (0.1% methylene blue), and imaged. For 3D assays, collagen or Matrigel gels containing fibroblasts (5 × 10^5 cells/ml) were prepared with plastic inserts placed in the gel center. After 24–48 h, the inserts were removed and the cell free space was filled with collagen containing 25 ng/ml PDGF, 100 μg/ml HA, and 25 ng/ml fibronectin. Gels were fixed and analyzed 72 h later.

Western blots

Western blots of CD44, phospho-ERK1,2, and total ERK1,2 proteins were performed as described previously (Schmits et al., 1997; Zhang et al., 1998; Tolg et al., 2003). Densitometry was performed using Image Quant 5.1 software (Molecular Dynamics).

Immunofluorescence of cultured cells

Immunofluorescence of phospho-ERK1,2 was done as described previously (Avizienyte et al., 2004). Immunofluorescence of CD44 and Rhamm was done using the same methods with overnight incubation of the primary antibodies at 4°C. Live-cell CD44 immunofluorescence was done as described previously (Robertson et al., 2006).

ERK1,2 assays

For quantification of serum or PDGF-induced ERK1,2 activation, cells were plated, serum starved, and stimulated with 10% FCS or PDGF as described. Western blots and immunofluorescence were done as described. The ERK1,2 ELISA was done according to the manufacturer's instructions.

Recombinant proteins and pull-down assays

Rhamm-GST (72-kD murine isoform) and GST recombinant proteins were prepared as described previously (Mohapatra et al., 1996). For pull-down assays, recombinant Rhamm-GST or GST beads were incubated with 500 μg of Rh^{FL}-rescued lysate overnight at 4°C. Beads were then washed with cold lysis buffer. Proteins associated with beads were boiled in SDS buffer and were detected by Western blot as described.

Excisional wounds and histology

Wt and Rh$^{-/-}$ mice were anaesthetized by Halothane inhalation. Two full-thickness 4-mm wounds were placed at the same location on denuded backs of age-matched male mice (9–18 mo), were harvested at the indicated times using an 8-mm metal punch, and were fixed and paraffin embedded as described previously (Tolg et al., 2003). To ensure that serial sections were cut starting at the wound center, samples were cut in half through the wound center before embedding. The first and last sections were stained with Masson's trichrome.

RT-PCR analysis of Rhamm mRNA

Rhamm mRNA was amplified from excised wound tissue, and PCR products were detected as described previously (Tolg et al., 2003). β-Actin was used as a loading control (Tolg et al., 2003).

Immunohistochemistry of tissue sections

Immunohistochemistry of paraffin processed sections was done as described previously (Tolg et al., 2003). Antigens were retrieved in 10 mM sodium citrate buffer, pH 6, heated to boiling, except for smooth muscle actin staining. Neutral lipids were detected in fixed cultured cells or frozen wound sections with 25 μg/ml BODIPY 493/503 (Invitrogen; Gocze and Freeman, 1994).

Image acquisition, image enhancement, image analysis, and statistical analysis

Masson's trichrome, hematoxylin and eosin, vimentin, tenascin, and phospho-ERK1,2 stained tissue section images were taken with air objectives (4×, NA 0.16; 20×, NA 0.7; Olympus) on a microscope (AX70 Provis; Olympus) with a color camera (Cooke SensiCam; CCD Imaging) and Image Pro Plus 4.5.1.2.9 (Media Cybernetics). Phospho-ERK1,2 staining was quantified with Photoshop 6.0 (Adobe). The area of blue (hematoxylin, total number of cells) was quantified. After deletion of the blue pixels, the peroxidase substrate (phospho-ERK1,2) was quantified. Tenascin staining was quantified using Simple PCI (Compix). Images in Fig. 9 A are composites of images taken with the 4× air objective. The colors were enhanced using Photoshop. Scratch wound and surface CD44 immunofluorescence images were taken with air objectives (4×, NA 0.1, and 20×, NA 0.4, respectively [Nikon], with Hoffman Modulation Contrast optics) using a microscope (Eclipse TE300; Nikon) with a digital camera (Hamamatsu) and Simple PCI software. In vivo wound images (Fig. S2 a) were taken with a digital camera (Dimage Z3; Minolta) with a 12× zoom. The wound area was quantified using Simple PCI. Confocal images were taken using an oil objective (63×, NA 1.4; Carl Zeiss MicroImaging, Inc.) with a confocal microscope (510 LSM Meta; Carl Zeiss MicroImaging, Inc.) using LSM 5 software (Carl Zeiss MicroImaging, Inc.). Fluorescence intensity of images was measured using LSM 5 software. Colocalization was identified and quantified using ImageJ software (http://rsb.info.nih.gov/ij/). Cell surface CD44 images were deconvolved using Simple PCI's nearest-neighbor

deconvolution. All images were acquired at room temperature. Unless otherwise indicated, comparisons between samples were assessed for statistical significance using a *t* test; P < 0.05 was considered significant, and significant differences between values are marked with asterisks.

Online supplemental material
Fig. S1 shows that transfection of Rh^{FL} into Rh$^{-/-}$ fibroblasts rescues defective migration in scratch wounds and invasion in collagen gel assays. Fig. S2 shows that Rhamm mRNA expression is transiently increased after excisional skin wounding between days 1 and 7. Photographs of wounds show that Rh$^{-/-}$ wounds contract more slowly than Wt. Tissue sections through excisional skin wounds confirm that loss of Rhamm results in significantly reduced wound contraction relative to Wt. Fig. S3 shows that the dermal structure of uninjured and repaired Rh$^{-/-}$ skin is aberrant compared with Wt. This includes alterations in dermal thickness and in differentiation of dermal cell types. Online supplemental material is available at http://www.jcb.org/cgi/content/full/jcb.200511027/DC1.

References

Adamia, S., C.A. Maxwell, and L.M. Pilarski. 2005. Hyaluronan and hyaluronan synthases: potential therapeutic targets in cancer. *Curr. Drug Targets Cardiovasc. Haematol. Disord.* 5:3–14.

Aitken, K., and D.J. Bagli. 2001. Stretch-induced bladder smooth muscle cell (SMC) proliferation is mediated by RHAMM-dependent extracellular-regulated kinase (erk) signaling. *Urology.* 57(Suppl. 1):109.

Avizienyte, E., V.J. Fincham, V.G. Brunton, and M.C. Frame. 2004. Src SH3/2 domain-mediated peripheral accumulation of Src and phospho-myosin is linked to deregulation of E-cadherin and the epithelial-mesenchymal transition. *Mol. Biol. Cell.* 15:2794–2803.

Bagli, D.J., B.D. Joyner, S.R. Mahoney, and L. McCulloch. 1999. The hyaluronic acid receptor RHAMM is induced by stretch injury of rat bladder in vivo and influences smooth muscle cell contraction in vitro. *J. Urol.* 162:832–840. (published erratum appears in *J. Urol.* 2003. 169:1090)

Bissell, M.J., and D. Radisky. 2001. Putting tumours in context. *Nat. Rev. Cancer.* 1:46–54.

Bissell, M.J., A. Rizki, and I.S. Mian. 2003. Tissue architecture: the ultimate regulator of breast epithelial function. *Curr. Opin. Cell Biol.* 15:753–762.

Bost, F., M. Aouadi, L. Caron, and B. Binetruy. 2005. The role of MAPKs in adipocyte differentiation and obesity. *Biochimie.* 87:51–56.

Bourguignon, L.Y., P.A. Singleton, H. Zhu, and B. Zhou. 2002. Hyaluronan promotes signaling interaction between CD44 and the transforming growth factor beta receptor I in metastatic breast tumor cells. *J. Biol. Chem.* 277:39703–39712.

Bourguignon, L.Y., E. Gilad, K. Rothman, and K. Peyrollier. 2005. Hyaluronan-CD44 interaction with IQGAP1 promotes Cdc42 and ERK signaling, leading to actin binding, Elk-1/estrogen receptor transcriptional activation, and ovarian cancer progression. *J. Biol. Chem.* 280:11961–11972.

Cheon, S.S., A.Y. Cheah, S. Turley, P. Nadesan, R. Poon, H. Clevers, and B.A. Alman. 2002. β-Catenin stabilization dysregulates mesenchymal cell proliferation, motility, and invasiveness and causes aggressive fibromatosis and hyperplastic cutaneous wounds. *Proc. Natl. Acad. Sci. USA.* 99:6973–6978.

Colucci-D'Amato, L., C. Perrone-Capano, and U. di Porzio. 2003. Chronic activation of ERK and neurodegenerative diseases. *Bioessays.* 25:1085–1095.

Crainie, M., A.R. Belch, M.J. Mant, and L.M. Pilarski. 1999. Overexpression of the receptor for hyaluronan-mediated motility (RHAMM) characterizes the malignant clone in multiple myeloma: identification of three distinct RHAMM variants. *Blood.* 93:1684–1696.

Evanko, S.P., W.T. Parks, and T.N. Wight. 2004. Intracellular hyaluronan in arterial smooth muscle cells: association with microtubules, RHAMM, and the mitotic spindle. *J. Histochem. Cytochem.* 52:1525–1535.

Filion, M.C., and N.C. Phillips. 2001. Pro-inflammatory activity of contaminating DNA in hyaluronic acid preparations. *J. Pharm. Pharmacol.* 53:555–561.

Gocze, P.M., and D.A. Freeman. 1994. Factors underlying the variability of lipid droplet fluorescence in MA-10 Leydig tumor cells. *Cytometry.* 17:151–158.

Goueffic, Y., C. Guilluy, P. Guerin, P. Patra, P. Pacaud, and G. Loirand. 2006. Hyaluronan induces vascular smooth muscle cell migration through RHAMM-mediated PI3K-dependent Rac activation. *Cardiovasc. Res.* 72:339–348.

Hall, C.L., B. Yang, X. Yang, X. Zhang, M. Turley, S. Samuel, L.A. Lange, C. Wang, G.D. Curpen, R.C. Savani, et al. 1995. Overexpression of the hyalruonan receptor RHAMM is transforming and is also required for H-ras transformation. *Cell.* 82:19–26.

Hall, C.L., L.A. Lange, D.A. Prober, S. Zhang, and E.A. Turley. 1996. pp60 (c-src) is required for cell locomotion regulated by the hyaluronanreceptor RHAMM. *Oncogene.* 13:2213–2224.

Hall, C.L., L.A. Collis, A.J. Bo, L. Lange, A. McNicol, J.M. Gerrard, and E.A. Turley. 2001. Fibroblasts require protein kinase C activation to respond to hyaluronan with increased locomotion. *Matrix Biol.* 20:183–192.

Hardwick, C., K. Hoare, R. Owens, H.P. Hohn, M. Hook, D. Moore, V. Cripps, L. Austen, D.M. Nance, and E.A. Turley. 1992. Molecular cloning of a novel hyaluronan receptor that mediates tumor cell motility. *J. Cell Biol.* 117:1343–1350.

Hascall, V.C., A.K. Majors, C.A. De La Motte, S.P. Evanko, A. Wang, J.A. Drazba, S.A. Strong, and T.N. Wight. 2004. Intracellular hyaluronan: a new frontier for inflammation? *Biochim. Biophys. Acta.* 1673:3–12.

Helfman, D.M., and G. Pawlak. 2005. Myosin light chain kinase and acto-myosin contractility modulate activation of the ERK cascade downstream of oncogenic Ras. *J. Cell. Biochem.* 95:1069–1080.

Hendriks, B.S., G. Orr, A. Wells, H.S. Wiley, and D.A. Lauffenburger. 2005. Parsing ERK activation reveals quantitatively equivalent contributions from epidermal growth factor receptor and HER2 in human mammary epithelial cells. *J. Biol. Chem.* 280:6157–6169.

Hofmann, M., C. Fieber, V. Assmann, M. Gottlicher, J. Sleeman, R. Plug, N. Howells, O. von Stein, H. Ponta, and P. Herrlich. 1998. Identification of IHABP, a 95 kDa intracellular hyaluronate binding protein. *J. Cell Sci.* 111:1673–1684.

Hornberg, J.J., B. Binder, F.J. Bruggeman, B. Schoeberl, R. Heinrich, and H.V. Westerhoff. 2005. Control of MAPK signalling: from complexity to what really matters. *Oncogene.* 24:5533–5542.

Huang, C., K. Jacobson, and M.D. Schaller. 2004. MAP kinases and cell migration. *J. Cell Sci.* 117:4619–4628.

Krueger, J.S., V.G. Keshamouni, N. Atanaskova, and K.B. Reddy. 2001. Temporal and quantitative regulation of mitogen-activated protein kinase (MAPK) modulates cell motility and invasion. *Oncogene.* 20:4209–4218.

Lokeshwar, V.B., and M.G. Selzer. 2000. Differences in hyaluronic acid-mediated functions and signaling in arterial, microvessel, and vein-derived human endothelial cells. *J. Biol. Chem.* 275:27641–27649.

Lovvorn, H.N., III, D.L. Cass, K.G. Sylvester, E.Y. Yang, T.M. Crombleholme, N.S. Adzick, and R.C. Savani. 1998. Hyaluronan receptor expression increases in fetal excisional skin wounds and correlates with fibroplasia. *J. Pediatr. Surg.* 33:1062–1069; discussion 1069–1070.

Marhaba, R., M. Bourouba, and M. Zoller. 2005. CD44v6 promotes proliferation by persisting activation of MAP kinases. *Cell. Signal.* 17:961–973.

Maxwell, C.A., J.J. Keats, M. Crainie, X. Sun, T. Yen, E. Shibuya, M. Hendzel, G. Chan, and L.M. Pilarski. 2003. RHAMM is a centrosomal protein that interacts with dynein and maintains spindle pole stability. *Mol. Biol. Cell.* 14:2262–2276.

Maxwell, C.A., J.J. Keats, A.R. Belch, L.M. Pilarski, and T. Reiman. 2005. Receptor for hyaluronan-mediated motility correlates with centrosome abnormalities in multiple myeloma and maintains mitotic integrity. *Cancer Res.* 65:850–860.

Mohapatra, S., X. Yang, J.A. Wright, E.A. Turley, and A.H. Greenberg. 1996. Soluble hyaluronan receptor RHAMM induces mitotic arrest by suppressing Cdc2 and cyclin B1 expression. *J. Exp. Med.* 183:1663–1668.

Nedvetzki, S., E. Gonen, N. Assayag, R. Reich, R.O. Williams, R.L. Thurmond, J.F. Huang, B.A. Neudecker, F.S. Wang, E.A. Turley, and D. Naor. 2004. RHAMM, a receptor for hyaluronan-mediated motility, compensates for CD44 in inflamed CD44-knockout mice: a different interpretation of redundancy. *Proc. Natl. Acad. Sci. USA.* 101:18081–18086.

Nickel, W. 2005. Unconventional secretory routes: direct protein export across the plasma membrane of mammalian cells. *Traffic.* 6:607–614.

Park, C.C., M.J. Bissell, and M.H. Barcellos-Hoff. 2000. The influence of the microenvironment on the malignant phenotype. *Mol. Med. Today.* 6:324–329.

Providence, K.M., and P.J. Higgins. 2004. PAI-1 expression is required for epithelial cell migration in two distinct phases of in vitro wound repair. *J. Cell. Physiol.* 200:297–308.

Radisky, D.C., Y. Hirai, and M.J. Bissell. 2003. Delivering the message: epimorphin and mammary epithelial morphogenesis. *Trends Cell Biol.* 13:426–434.

Reid, R.R., H.K. Said, J.E. Mogford, and T.A. Mustoe. 2004. The future of wound healing: pursuing surgical models in transgenic and knockout mice. *J. Am. Coll. Surg.* 199:578–585.

Robertson, S.E., S.R. Setty, A. Sitaram, M.S. Marks, R.E. Lewis, and M.M. Chou. 2006. Extracellular signal-regulated kinase regulates clathrin-independent endosomal trafficking. *Mol. Biol. Cell.* 17:645–657.

Samuel, S.K., R.A. Hurta, M.A. Spearman, J.A. Wright, E.A. Turley, and A.H. Greenberg. 1993. TGF-β1 stimulation of cell locomotion utilizes the hyaluronan receptor RHAMM and hyaluronan. *J. Cell Biol.* 123:749–758.

Schmits, R., J. Filmus, N. Gerwin, G. Senaldi, F. Kiefer, T. Kundig, A. Wakeham, A. Shahinian, C. Catzavelos, J. Rak, et al. 1997. CD44 regulates hemato-poietic progenitor distribution, granuloma formation, and tumorigenicity. *Blood.* 90:2217–2233.

Simoes, R.L., and I.M. Fierro. 2005. Involvement of the Rho-kinase/myosin light chain kinase pathway on human monocyte chemotaxis induced by ATL-1, an aspirin-triggered lipoxin A4 synthetic analog. *J. Immunol.* 175:1843–1850.

Tolg, C., R. Poon, R. Fodde, E.A. Turley, and B.A. Alman. 2003. Genetic deletion of receptor for hyaluronan-mediated motility (Rhamm) attenuates the formation of aggressive fibromatosis (desmoid tumor). *Oncogene.* 22:6873–6882.

Toole, B.P. 2004. Hyaluronan: from extracellular glue to pericellular cue. *Nat. Rev. Cancer.* 4:528–539.

Travis, J.A., M.G. Hughes, J.M. Wong, W.D. Wagner, and R.L. Geary. 2001. Hyaluronan enhances contraction of collagen by smooth muscle cells and adventitial fibroblasts: role of CD44 and implications for constrictive remodeling. *Circ. Res.* 88:77–83.

Turley, E.A. 1982. Purification of a hyaluronate-binding protein fraction that modifies cell social behavior. *Biochem. Biophys. Res. Commun.* 108:1016–1024.

Turley, E.A., L. Austen, D. Moore, and K. Hoare. 1993. Ras-transformed cells express both CD44 and RHAMM hyaluronan receptors: only RHAMM is essential for hyaluronan-promoted locomotion. *Exp. Cell Res.* 207:277–282.

Turley, E.A., P.W. Noble, and L.Y. Bourguignon. 2002. Signaling properties of hyaluronan receptors. *J. Biol. Chem.* 277:4589–4592.

Wang, C., J. Entwistle, G. Hou, Q. Li, and E.A. Turley. 1996. The characterization of a human RHAMM cDNA: conservation of the hyaluronan-binding domains. *Gene.* 174:299–306.

Watanabe, T., J. Noritake, and K. Kaibuchi. 2005. Regulation of microtubules in cell migration. *Trends Cell Biol.* 15:76–83.

Yao, Y., W. Li, J. Wu, U.A. Germann, M.S. Su, K. Kuida, and D.M. Boucher. 2003. Extracellular signal-regulated kinase 2 is necessary for mesoderm differentiation. *Proc. Natl. Acad. Sci. USA.* 100:12759–12764.

Zaman, A., Z. Cui, J.P. Foley, H. Zhao, P.C. Grimm, H.M. Delisser, and R.C. Savani. 2005. Expression and role of the hyaluronan receptor RHAMM in inflammation after bleomycin injury. *Am. J. Respir. Cell Mol. Biol.* 33:447–454.

Zhang, S., M.C. Chang, D. Zylka, S. Turley, R. Harrison, and E.A. Turley. 1998. The hyaluronan receptor RHAMM regulates extracellular-regulated kinase. *J. Biol. Chem.* 273:11342–11348.